Physics of the Solid State, Vol. 42, No. 5, 2000, pp. 810–815. Translated from Fizika Tverdogo Tela, Vol. 42, No. 5, 2000, pp. 791–796.

METALS AND SUPERCONDUCTORS

Transport Properties of HTSC + Ba(Pb, Met)O_3 Composites as Functions of the Electrical and Magnetic Characteristics of Nonsuperconducting Components

M. I. Petrov, D. A. Balaev, S. V. Ospishchev, and K. S. Aleksandrov

Kirenskiĭ Institute of Physics, Siberian Division, Russian Academy of Sciences, Akademgorodok, Krasnoyarsk, 660036 Russia

e-mail: smp@iph.krasnoyarsk.su

Received in final form October 26, 1999

Abstract—Composites simulating a network of weak metallic links and consisting of a classic 1–2–3 HTSC and a $BaPbO_3$ metal oxide with incorporated Sn, Ni, and Fe impurities have been prepared. Experimental resistivity, magnetic, and Mössbauer studies of the $BaPb_{0.9}Met_{0.1}O_3$ nonsuperconducting components are presented. The transport properties of the HTSC + $BaPb_{0.9}Met_{0.1}O_3$ composites have been investigated. The superconducting properties of the composites are observed to be suppressed, both when the carrier mean free path in nonsuperconducting components with tin impurities decreases, and as a result of an additional interaction of the magnetic moments of (Fe, Ni) impurities with the spins of supercurrent carriers. The experimental temperature dependences of the composite critical current are analyzed in terms of the de Gennes theory for the superconductor–normal metal–superconductor structures. © *2000 MAIK "Nauka/Interperiodica".*

As shown in our earlier experimental study [1], HTSC + $BaPbO_3$ composites are equivalent to an *S–N–S* weak-link network (*S* stands here for a superconductor, and *N*, for a normal metal) in the "clean" limit. Indeed, the mean free path l in $BaPbO_3$ is substantially longer than the coherence length ξ_0 in HTSCs, and this accounts for the fact that the theory [2], including in the clean limit the tunneling, the proximity effect, and Andreev scattering, provides a good description of the transport properties of these composites. The part played by weak links in an *S–N–S* structure can, however, be varied by properly varying not only the effective thickness of the *N* layer (a subject of study in [1, 3]), but the mean free path of carriers in the normal metal *N* as well.

The dependence of the critical current of *S–N–S* junctions on the thickness of the *N* layer, as well as on the carrier mean free path in it, was studied comprehensively for low-temperature superconductors [4]. The mean free path and the nature of interaction of impurities with Cooper pairs were varied by introducing impurities, both nonmagnetic and paramagnetic, into the *N* metal. The BCS-based theory was found to agree with the experiment; however, one did not measure and, hence, analyze the temperature dependences of the critical current.

By analogy with [4], we have made an attempt to carry out a similar study on HTSC-based *S–N–S* structures. Unfortunately, the absence of a reproducible technology of manufacturing single junctions forced us to study HTSC + normal metal composites. As already mentioned, such composites are equivalent to a weak-link network characterized by some distribution function of the *S–N–S* junctions (links) in this network in their geometrical parameters. However, if the technology of composite preparation is followed with a good enough reproducibility, it appears logical to expect the distribution function to be reproducible and to associate all variations in the transport properties with the interaction of supercurrent carriers tunneling through a metal with various impurities.

The specific difficulties involved in the preparation of HTSC-based composites are considered partially in [1, 3]. One of them, namely, the oxidation of the *N* metal, was overcome by using the $BaPbO_3$ metal oxide, which exhibits only a weak chemical interaction with 1–2–3 HTSCs [1, 3]. Our preliminary experiments [5] showed that incorporating impurities in $BaPbO_3$ brings about a noticeable additional degradation of the superconducting properties of the *S–N–S* weak-link network in HTSC + $BaPbO_3$ composites.

This work presents detailed experimental data on a study of the effect of magnetic (Fe, Ni) and nonmagnetic (Sn) impurities introduced into $BaPbO_3$ on the transport properties of HTSC + Ba(Pb, Met)O_3 composites.

1. PREPARATION AND PHYSICAL PROPERTIES OF NONSUPERCONDUCTING COMPONENTS

The nonsuperconducting components of the composites were prepared of the BaO_2, PbO, NiO, $Fe_2^{57}O_3$, and $Sn^{119}O_2$ oxides at 880°C by ceramic technology. Using the hematite enriched in the Fe^{57} isotope to 90%

1063-7834/00/4205-0810$20.00 © 2000 MAIK "Nauka/Interperiodica"

made monitoring the solubility of iron in $BaPbO_3$ by Mössbauer spectroscopy (Fig. 1) possible. Annealing for two weeks, alternating with grinding, is seen to result in the disappearance of the six-line spectrum of the $Fe_2^{57}O_3$ hematite, which is evidence of its "dissolution" in $BaPbO_3$. To increase the reliability still further, the synthesis was prolonged for one more week. The $BaPb_{0.9}Ni_{0.1}O_3$ and $BaPb_{0.9}Sn_{0.1}O_3$ sample were prepared by the technique used to synthesize the iron-containing $BaPbO_3$. The "dissolution" of tin in $BaPbO_3$ was also checked by Sn^{119} Mössbauer spectroscopy. The absence of a spectrum characteristic of SnO_2 argues for complete "dissolution" of tin in $BaPbO_3$. There is nothing strange in this, because Sn^{4+} is an electronic analog of Pb^{4+}. X-ray diffraction analysis performed on $BaPb_{0.9}Met_{0.1}O_3$ samples revealed the $BaPbO_3$ perovskite phase, with no foreign reflections evident within the analytical accuracy.

Figure 2 presents temperature dependences of the electrical resistivity $\rho(T)$ of $BaPb_{0.9}Met_{0.1}O_3$ and $BaPbO_3$ samples measured by the four-point probe method. Partial substitution of lead makes the $\rho(T)$ curves only weakly dependent on temperature (with a slight increase of ρ, with decreasing temperature observed for the $BaPb_{0.9}Fe_{0.1}O_3$ sample), and results in an increase of ρ in an absolute magnitude, it being the largest for the iron impurities (see the table). This is not at odds with the classical mechanism of carrier interaction with magnetic and nonmagnetic impurities [6].

Figure 3 illustrates magnetic measurements made on samples with Ni and Fe impurities. The measurements were carried out on a vibrating-sample magnetometer [7]. A comparison of the experimental magnetization curve $M(H)$ with the Brillouin function permitted determination of the magnetic moments per impurity atom. The best-fit figures are 3.6 μB for Fe and 0.13 μB for Ni ions (μB is the Bohr magneton). The value for the iron ions is slightly smaller than the nominal value for Fe^{4+} [8], if one assumes that the cations of iron to substitute for those of lead in the $BaPbO_3$ structure. As for nickel, one may conjecture Ni to also occupy the lead sites in $BaPbO_3$, which makes +4 its formal valence state. In this case, the electronic configuration of the Ni^{4+} cation should be $3d^6$. Assuming this configuration, the low-spin state (no high-spin state was ever observed for Ni^{4+} [9]) yields zero spin magnetic moment. By contrast, the experimental value is 0.13 μB. A possible reason for the nonzero magnetic moment of Ni could be a covalent admixture to the nickel 3*d* levels. Thus, the magnetic moment for both the iron and nickel in the metal oxide is seen to deviate from the nominal value, which is in marked contrast with the behavior of magnetodielectrics, where this agreement is much better [8].

The magnetization of the samples drops with increasing temperature by the $1/T$ law, which argues for

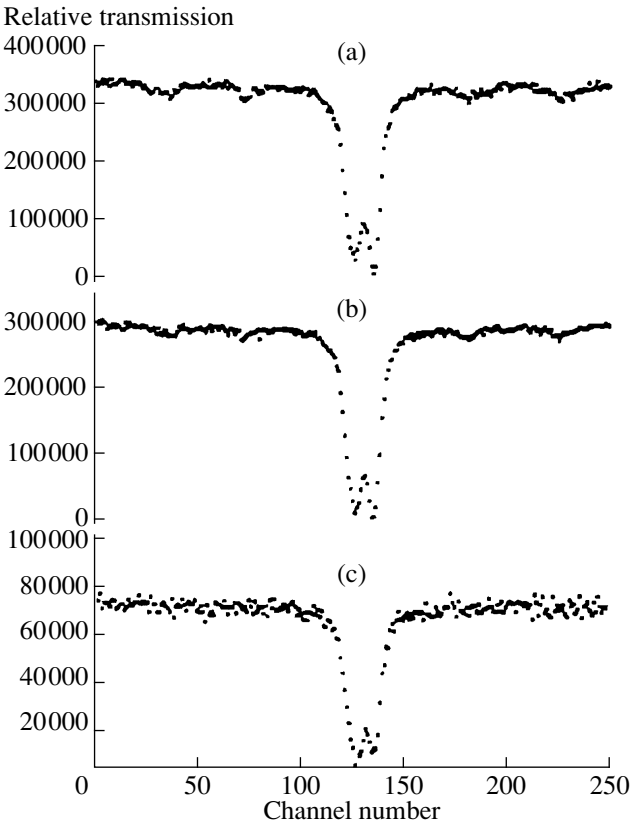

Fig. 1. Mössbauer spectra of $BaPb_{0.9}Fe_{0.1}^{57}O_3$. (a) After one weak of synthesis, (b) after two weeks, (c) after three weeks.

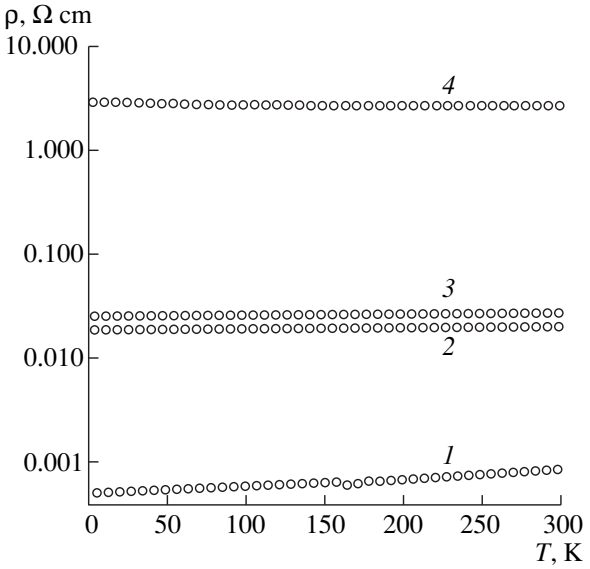

Fig. 2. Experimental $\rho(T)$ relations for the nonsuperconducting components of the composites plotted on a semilogarithmic scale. (*1*) $BaPbO_3$, (*2*) $BaPb_{0.9}Sn_{0.1}O_3$, (*3*) $BaPb_{0.9}Ni_{0.1}O_3$, (*4*) $BaPb_{0.9}Fe_{0.1}O_3$.

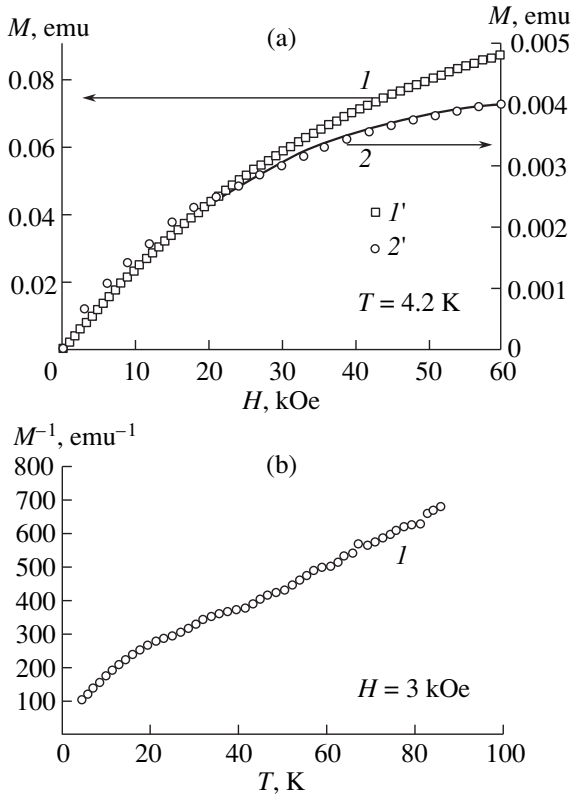

Fig. 3. Magnetic measurements on nonsuperconducting components of the composites (*1*') $BaPb_{0.9}Fe_{0.1}O_3$ (m = 96 mg) and (*2*') $BaPb_{0.9}Ni_{0.1}O_3$ (m = 112 mg). (a) Field dependences (for T = 4.2 K), (b) temperature dependences (for H = 3 kOe) of the magnetization M. Solid curves represent calculations made using the Brillouin function with (*1*) J = 1 for $BaPb_{0.9}Fe_{0.1}O_3$ and (*2*) J = 2 for $BaPb_{0.9}Ni_{0.1}O_3$.

the compounds being paramagnetic (see Fig. 3). The absence of a hysteresis in the field dependences bears out this assumption. The deviation of the $M^{-1} = f(T)$ relation from a linear course in the low-temperature domain suggests that one should take into account pairwise exchange interactions; however, this work does not deal with a study of the various aspects of the magnetism of these compounds, but rather of the effect of magnetic scattering centers on the transport properties of composites containing them.

2. PREPARATION AND TRANSPORT PROPERTIES OF THE HTSC + Ba(Pb, Met)O_3 COMPOSITES

The superconducting component of the composites, $Y_{0.75}Lu_{0.25}Ba_2Cu_3O_7$, was prepared by the standard ceramic technology. The composites were synthesized by fast sintering [1, 3]. The composite components, mixed thoroughly in the ratio 85 vol % HTSC with 15 vol % $BaPb_{0.9}Met_{0.1}O_3$ (Met = Sn, Ni, Fe), were pressed into pellets, placed onto preheated boats, and introduced for five minutes into a furnace heated to 950°C. Because a 1–2–3 HTSC inevitably loses oxygen at this temperature, the composite samples were transferred from this high-temperature furnace to another furnace maintained at 400°C in order to restore the oxygen stoichiometry, where they were kept for six hours, which is long enough to reach oxygen saturation [1].

To learn the effect of various impurities present in the nonsuperconducting component on the transport properties of the composites, the results obtained were compared with the data for a reference composite that did not contain impurities in $BaPbO_3$.

X-ray diffraction analysis of the composites revealed the presence of two phases only, the 1–2–3 HTSC and the perovskite. No other reflections were detected within the analytical errors.

Denote the composite samples by S + 15N, S + 15N(Sn10), S + 15N(Ni10), and S + 15N(Fe10). Here S stands for the superconductor, N, for the impurity-free $BaPbO_3$, and N(Sn10), N(Ni10), N(Fe10), for $BaPb_{0.9}Met_{0.1}O_3$ with Met = Sn, Ni, and Fe, respectively.

The temperature dependences of the composite magnetization, $M(T)$, measured in a field of 200 Oe, showed the presence of one superconducting phase at temperatures below 93.5 K. The $M(T)$ relations are similar in pattern to those quoted in [10] for the HTSC + $BaPbO_3$ composites.

Figure 4 illustrates the effect of the various impurities in $BaPbO_3$ on the I–V characteristics of the composites at T = 4.2 K. The I–V relations were measured by the four-point probe technique, with the sample placed directly into a helium bath for efficient heat

Some parameters of the composite nonsuperconducting components

N-metal	μ, μ_0	ρ(5 K), Ω cm	R_N, Ω cm	l, Å	T_{pb}, K
$BaPbO_3$	–	0.0005	0.0022	>100	0
$BaPb_{0.9}Sn_{0.1}O_3$	–	0.019	0.0089	4.4 ± 1.0	0
$BaPb_{0.9}Ni_{0.1}O_3$	0.13	0.026	0.0098	4.0 ± 0.5	20 ± 5
$BaPb_{0.9}Fe_{0.1}O_3$	3.6	3.0	0.0524	4.0 ± 0.5	50 ± 5

Note: μ is the magnetic moment per impurity atom, ρ is the electrical resistivity, R_N is the normal resistance of composites with the corresponding components at T = 4.2 K. The values of l and T_{pb} were derived from the best fit of the experimental $J_c(T)$ relations for the composites to the de Gennes theory (see Sect. 3).

removal (for more details, see [11, 12]). The I–V characteristics shown in Fig. 4 exhibit an extra current, which is typical of *S*–*N*–*S* structures [13]. The table lists the normal resistances R_N of the composites, derived from the linear part of the I–V characteristics at $T = 4.2$ K. The values of ρ of the components correlate clearly with R_N.

Figure 5 presents normalized temperature dependences of the electrical resistance $R(T)$ of the composites, measured by the four-point probe technique for a transport current of $\sim 0.01 \times J_c(5\ \mathrm{K})$ [$J_c(5\ \mathrm{K})$ is the critical current at 5 K]. The jump in the electrical resistance at 93.5 K corresponds to the HTSC grains undergoing the superconducting transition in the composite. The fact that this temperature is the same for all the composite samples argues against diffusion of chemical elements from the nonsuperconducting components into the HTSC grains. The smooth tail in the $R(T)$ relations seen below 93.5 K is due to the weak links [1, 3, 10, 14–16]. The characteristic temperature at which the resistance of a composite sample becomes zero depends on the nature of the impurity introduced in $BaPbO_3$ (see Fig. 5). The $R(T)$ curve for the composites containing magnetic impurities has a segment below the T_c of the HTSC grains, extended in temperature, within which the resistance varies only weakly, with a subsequent transition to the superconducting state. Such $R(T)$ behavior was observed in $YBa_2Cu_3O_7/Pr_{0.7}Sr_{0.3}MnO_3/Ag$ and $YBa_2Cu_3O_7/Pr_{0.7}Sr_{0.3}MnO_3/YBa_2Cu_3O_7$ sandwiches with a ferromagnetic interlayer [14], as well as in HTSC + CuO-insulator composites with magnetic scattering centers (Ni) [15]. This behavior is apparently accounted for by the interaction of carrier pairs with magnetic moments in the interlayers.

The temperature dependences of the critical current density $J_c(T)$ of the composites measured by the four-point probe technique based on a standard 1 μV/cm criterion [17] (with the method employed described in detail in [1, 10]) are displayed in Fig. 6. Note certain features in the experimental $J_c(T)$ relations. Although the curves follow the same pattern for all the samples, the absolute values of $J_c(5\ \mathrm{K})$ for the composites depend strongly on the character of the impurity (Sn, Ni, Fe) and correlate with the electrical resistance data. For high temperatures, the experimental values of $J_c(T)$ become extremely small, and at a finite measuring-current density [$\sim 0.01 \times J_c(5\ \mathrm{K})$] a nonzero voltage drop appears (Figs. 5, 6).

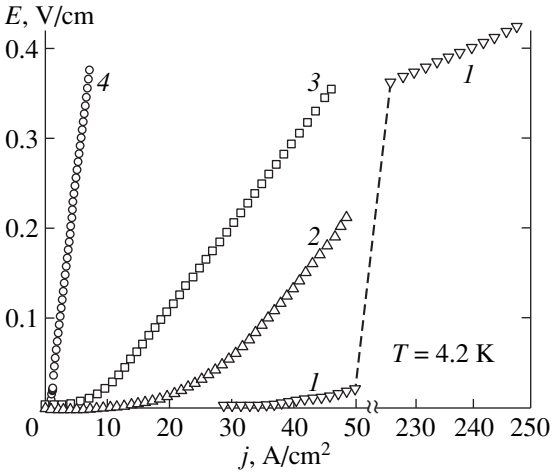

Fig. 4. Experimental I–V characteristics of composite samples obtained at $T = 4.2$ K. (*1*) *S* + 15*N*, (*2*) *S* + 15*N*(Sn10), (*3*) *S* + 15*N*(Ni10), (*4*) *S* + 15*N*(Fe10).

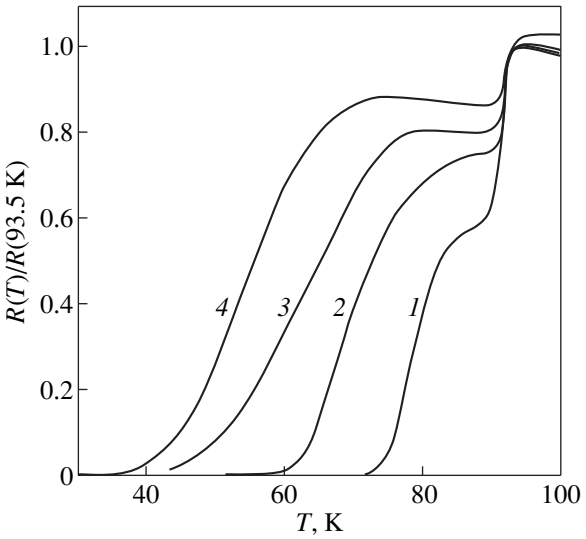

Fig. 5. Experimental temperature dependences of the electrical resistance of the samples. (*1*) *S* + 15*N*, (*2*) *S* + 15*N*(Sn10), (*3*) *S* + 15*N*(Ni10), (*4*) *S* + 15*N*(Fe10).

3. ANALYSIS OF THE TEMPERATURE BEHAVIOR OF CRITICAL CURRENT FOR THE HTSC + Ba(Pb, Met)O_3 COMPOSITES

As shown by an analysis of the $J_c(T)$ relations for the HTSC + $BaPbO_3$ composites [1, 10], a composite sample can be characterized by an average geometrical weak-link length *d*. For the 15 vol % $BaPbO_3$ samples, this value, estimated by the theory of [2], was found to be ~100 Å. It was natural to expect that the value of *d* for the composites with impurities in $BaPbO_3$, prepared by the same technology and with the same content of the nonsuperconducting component, would be the same.

Unfortunately, there is presently no microscopic theory applicable to the temperature dependence of the critical current for the crossover from the "clean" limit ($l > d_{\mathrm{eff}}$, where d_{eff} is the effective weak-link length [18]) to the "dirty" one ($l \ll d_{\mathrm{eff}}$ [18]), like this was done for the I–V characteristics of *S*–*N*–*S* junctions [19, 20]. Therefore we are going to present here the results of a

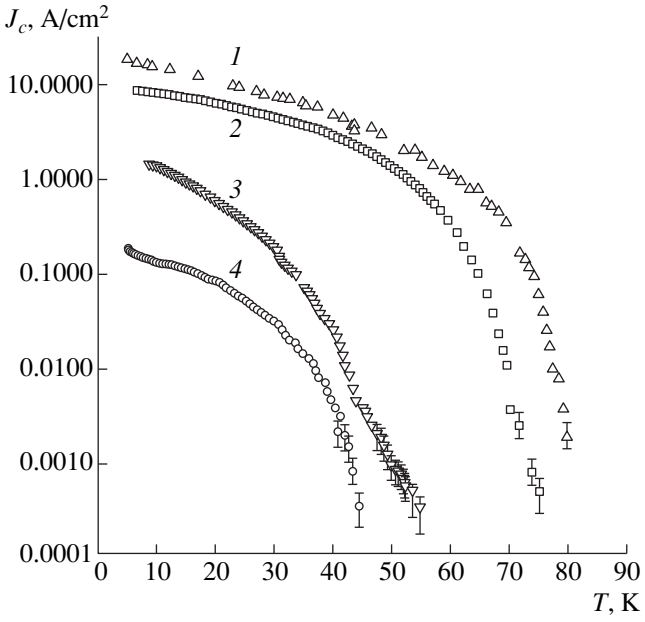

Fig. 6. Experimental temperature dependences of the critical current density of composites drawn on a semilogarithmic scale. (*1*) *S* + 15*N*, (*2*) *S* + 15*N*(Sn10), (*3*) *S* + 15*N*(Ni10), (*4*) *S* + 15*N*(Fe10).

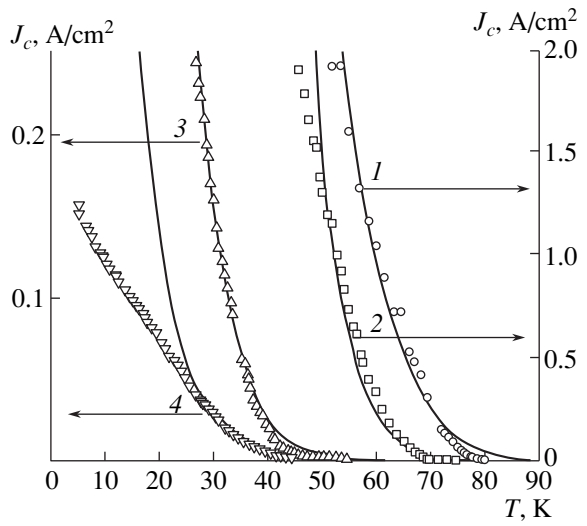

Fig. 7. Temperature dependences of the critical current. (*1*) *S* + 15*N*, (*2*) *S* + 15*N*(Sn10), (*3*) *S* + 15*N*(Ni10), (*4*) *S* + 15*N*(Fe10). Solid curves are fits plotted by the de Gennes theory (see text and the table).

treatment of the experimental $J_c(T)$ relations made on the basis of the de Gennes proximity theory [21].

At temperatures not too far from T_c, the de Gennes theory yields for the critical current of a *S*–*N*–*S* junction [17, 22, 23]

$$J_c(T) = C(1 - T/T_c)^2 \frac{d/\xi N}{\sinh(d/\xi N)}, \qquad (1)$$

where C is a constant that depends on the contact geometry, which for a three-dimensional network of Josephson junctions with some distribution function for the geometric parameters plays the part of a normalization factor, d is the geometric width of the N interlayer, which is an effective quantity for composites, and ξ_N is the coherence length in the N metal or the pair penetration depth into the N metal, which for a "dirty" N metal is defined as [17, 22]

$$\xi_N = (\hbar V_f l/6\pi k_B T)^{1/2}, \qquad (2)$$

where $\hbar$ is the Planck constant, k_B is the Boltzmann constant, and V_f is the Fermi velocity in the N metal. If the N interlayer is not a "clean" metal, ξ_N does not depend on the mean free path and is defined as [22]

$$\xi_N = \hbar V_f/2\pi k_B T. \qquad (3)$$

The fitting parameters for experimental $J_c(T)$ curves are d and l; besides, one should also know V_f. The best fit of the theory to the experiment was reached for $V_f \approx 1.8 \times 10^7$ cm/s, the value derived from the relation $V_f = \hbar \times 3^{1/3}\pi^{2/3} n^{1/3}$ m^{-1} (m is the electron mass) for $n = 1.4 \times 10^{20}$ cm^{-3} quoted in [24] for $BaPbO_3$.[1]

The best-fit curve for the experimental $J_c(T)$ relation obtained for the *S* + 15*N* sample (curve *1* in Fig. 7) within the 55–80-K temperature interval was calculated using (3) and (1) for $d = 100$ Å.

The curve for the case of nonmagnetic impurities was calculated from (2) and (1). We tried to fit the experimental data for the sample *S* + 15*N*(Sn10) (curve *2* in Fig. 7) to the theory in the high-temperature region [15–20 K below the temperature at which $J_c(T)$ becomes practically zero] by varying the mean free path in (2). The best fit was reached at a surprisingly small value of 4.4 ± 1 Å. At the same time, straightforward calculations show that at a tin concentration $x = 0.125$, the most probable distance between scattering centers (Sn atoms) in $BaPb_{1-x}Sn_xO_3$ is equal to the lattice constant 4.268 Å; for $x = 0.1$, it is 4.6 Å, which is close to the estimate of l obtained here.

While the de Gennes theory could formally be used to treat the $J_c(T)$ curves for samples with magnetic impurities in $BaPbO_3$ (in Fig. 7, these relations extend to lower temperatures), and the mean free paths thus obtained would obviously be substantially less than the lattice constant, which is an unphysical result. This is a consequence of the fact that the de Gennes theory does not include the mechanism of Cooper pair interaction with the magnetic moments of the N interlayer. In our opinion, an original way out of this problem was pro-

[1] In the case of the Sn ⟶ Pb substitution, there are no grounds to expect n to change, because tin has the same electronic configuration as lead. The change in n caused by a nickel and iron substitution should not apparently be larger than that for $BaPb_{1-x}BiO_3$ [24–26] and, because of the $V_f(n) \sim n^{1/3}$ dependence being weak, should only slightly affect the results of the fitting given in the table.

posed in [22], where the mean lifetime τ of a pair inside the N interlayer is modified to become

$$\tau = \tau + \tau_{pb} = (\hbar/2\pi k_B)(1/T + 1/T_{pb}) \qquad (4)$$

(we are using here the notation accepted in [22]). The effect of this mechanism on the critical current consists in substituting $T + T_{pb}$ for T in (3). Curves *3* and *4* in Fig. 7, which are the best fits to $J_c(T)$ for the samples $S + 15N$(Ni10) and $S + 15N$(Fe10), were calculated using expressions (1), (2), and (4) with the parameters given in the table.

At low temperatures, one observes a noticeable discrepancy between the experiment and the de Gennes theory, which is illustrated in Fig. 7 for the $S + 15N$(Fe10) sample. Similar cases were reported by other authors as well [22, 23], which is hardly surprising, because, as already pointed out above, the theory of the proximity effect was developed for the high-temperature domain [21, 22].

Summing up the results obtained in this work, we note that magnetic impurities degrade the transport properties of composites more strongly than nonmagnetic ones do. This degradation is more pronounced in the case where the impurity is the iron atoms, whose magnetic moment is substantially higher than that of the nickel atoms. The degradation of superconductivity in $BaPbO_3$ having a tin impurity can be associated only with a decrease of the carrier mean free path in the N layer. In the case of composites with $BaPbO_3$ containing magnetic impurities, this degradation of the superconducting properties can be related to one more mechanism of Cooper pair breaking, namely, through the exchange interaction at impurity magnetic moments [4].

This Cooper-pair breaking by impurities can be connected with inelastic processes, such as magnetic scattering in conventional *s*-type superconductors. In *d*-type superconductors, however, strong elastic scattering can also bring about pair breaking, as this was pointed out in [23].

ACKNOWLEDGMENTS

The authors are indebted to A.D. Balaev for his assistance in magnetic measurements and for fruitful discussions, to O.A. Bayukov for Mössbauer measurements, and to A.D. Vasil'ev for x-ray diffraction studies. We are also grateful to Prof. Kümmel (Universität Würzburg, Germany) for his interest in this work. One of us, D. A. Balaev, is grateful to Prof. Nicolsky (Instituto de Fisica, Universidade Federal do Rio de Janeiro, Brazil), for stimulating discussions.

Partial support from the Young Scientists' Foundation, Siberian Division of the Russian Academy of Sciences, for 1998–1999, is gratefully acknowledged.

REFERENCES

1. M. I. Petrov, D. A. Balaev, S. V. Ospishchev, *et al.*, Phys. Lett. A **237**, 85 (1997).
2. U. Gunsenheimer, U. Schüssler, and R. Kümmel, Phys. Rev. B **49**, 6111 (1994).
3. M. I. Petrov, D. A. Balaev, S. V. Ospishchev, *et al.*, Fiz. Tverd. Tela (St. Petersburg) **39** (3), 418 (1997) [Phys. Solid State **39**, 362 (1997)].
4. J. Niemeyer and G. von Minnegerode, Z. Physik B **36**, 57 (1979).
5. M. I. Petrov, D. A. Balaev, S. V. Ospishchev, *et al.*, Physica C **282**–**287**, 2447 (1997).
6. A. A. Abrikosov, *Introduction to the Theory of Normal Metals* (Nauka, Moscow, 1972).
7. A. D. Balaev, Yu. V. Boyarshinov, M. M. Karpenko, *et al.*, Prib. Tekh. Éksp. **3**, 167 (1985).
8. S. Krupićka, *Physik der Ferrite und der verwandten magnetischen Oxide* (Academia, Prague, 1973; Mir, Moscow, 1976), Vol. 1.
9. F. A. Cotton and G. Wilkinson, *Advanced Inorganic Chemistry* (Wiley, New York, 1966), Vols. 1–3.
10. M. I. Petrov, D. A. Balaev, B. P. Khrustalev, *et al.*, Sverkhprovod.: Fiz., Khim., Tekh. **8** (1), 53 (1995).
11. M. I. Petrov, S. N. Krivomasov, B. P. Khrustalev, *et al.*, Solid State Commun. **82**, 453 (1992).
12. M. I. Petrov, D. A. Balaev, D. M. Gohfeld, *et al.*, Physica C **314**, 51 (1999).
13. G. E. Blonder, M. Tinkham, and T. M. Klapwijk, Phys. Rev. B **25**, 4515 (1982).
14. G. C. Xiong, G. J. Lian, J. F. Kang, *et al.*, Physica C **282**–**287**, 693 (1997).
15. M. I. Petrov, D. A. Balaev, K. A. Shaĭkhutdinov, *et al.*, Fiz. Tverd. Tela (St. Petersburg) **40** (9), 1599 (1998) [Phys. Solid State **40**, 1451 (1998)].
16. A. Gerber, T. Grenet, M. Cyrot, *et al.*, Phys. Rev. Lett. **65**, 3201 (1990).
17. A. Barone and G. Paterno, *Physics and Applications of the Josephson Effect* (Wiley, New York, 1982; Mir, Moscow, 1984).
18. K. K. Likharev, Rev. Mod. Phys. **51** (1), 101 (1979).
19. R. Kümmel, B. Huckestein, and R. Nicolsky, Solid State Commun. **65**, 1567 (1988).
20. R. Kümmel, U. Gunsenheimer, and R. Nicolsky, Phys. Rev. B **42**, 3992 (1990).
21. P. G. de Gennes, Rev. Mod. Phys. **36**, 225 (1964).
22. L. Antogonazza, S. J. Berkowitz, T. H. Geballe, *et al.*, Phys. Rev. B **51** (13), 8560 (1995).
23. K. Char, Physica C **282**–**287**, 419 (1997).
24. K. Kitazawa, A. Katsui, A. Toriumi, *et al.*, Solid State Commun. **52**, 459 (1984).
25. T. D. Thanh, A. Koma, and S. Tanaka. Appl. Phys. **22**, 205 (1980).
26. D. P. Moiseev, S. K. Uvarova, and M. B. Fenik, Fiz. Tverd. Tela (Leningrad) **23** (8), 2347 (1981) [Sov. Phys. Solid State **23**, 1371 (1981)].

Translated by G. Skrebtsov